Supplemental Figure Legends

Supplemental Figure 1

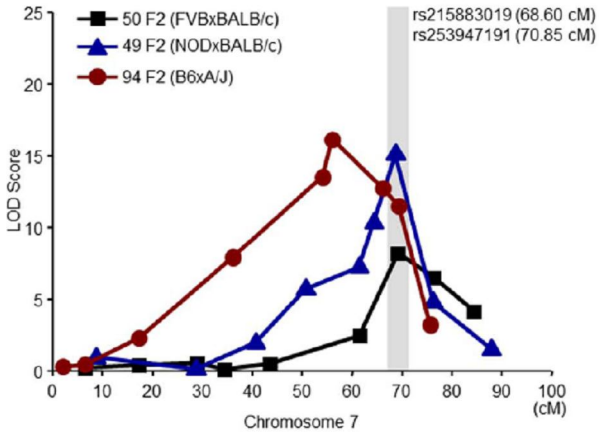

Fine-mapping and characterization of the *Canq1* locus. *Canq1* was mapped to distal chromosome 7 by linkage analyses in multiple F2 intercross populations (FVB x BALB/c, NOD x BALB/c, and B6 x A/J). Three markers, rs31386905 (69.13 cM), D7Mit68 (68.76 cM), and D7Mit130 (57.52 cM), are located at the peaks of FVB x BALB/c, NOD x BALB/c, and B6 x A/J, respectively. The genomic region (68.60 cM ~ 70.85 cM) on distal chromosome 7 with grey box indicates the region of statistical significance identified through haplotype association analysis of *Civq1* and *Canq1* across multiple inbred strains. This locus overlaps *Civq1* (Reference genome: NCBI Build 38).

Supplemental Figure 2

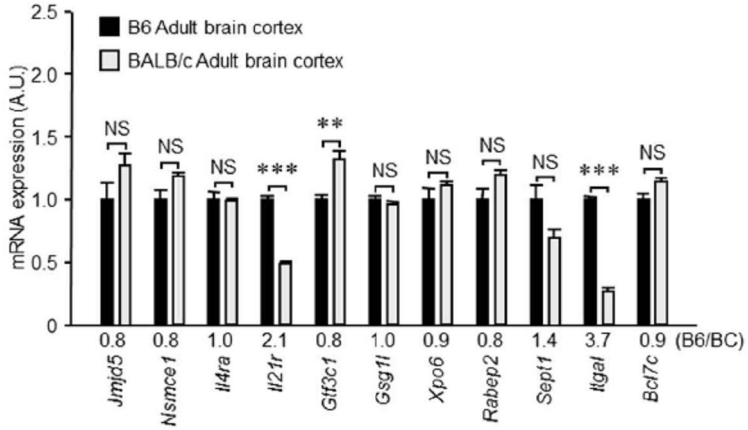

Strain-specific trancript levels of the candidate genes. Levels of each gene transcript in adult (12 week) brain cortex from B6 and BALB/c were determined by qRT-PCR. *Gapdh* was used for normalization. Values represent mean ± SEM from 6 animals per B6 and 7 animals per BALB/c (** $p<.01$ and *** $p<.001$, by 2-tailed Student's *t* test).

Supplemental Figure 3

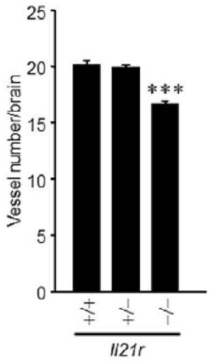

Collateral vessel connections between the MCA and PCA. The average number of collateral vessel connections between the MCA and PCA are shown. The total number of animals for *Il21r* WT, *Il21r* Het, and *Il21r* KO are 12, 6, and 16 animals, respectively. Values represent the mean ± SEM (*** *p<.001 vs. Il21r* WT and *Il21r* Het, by 2-tailed Student's *t* test).

Supplemental Figure 4

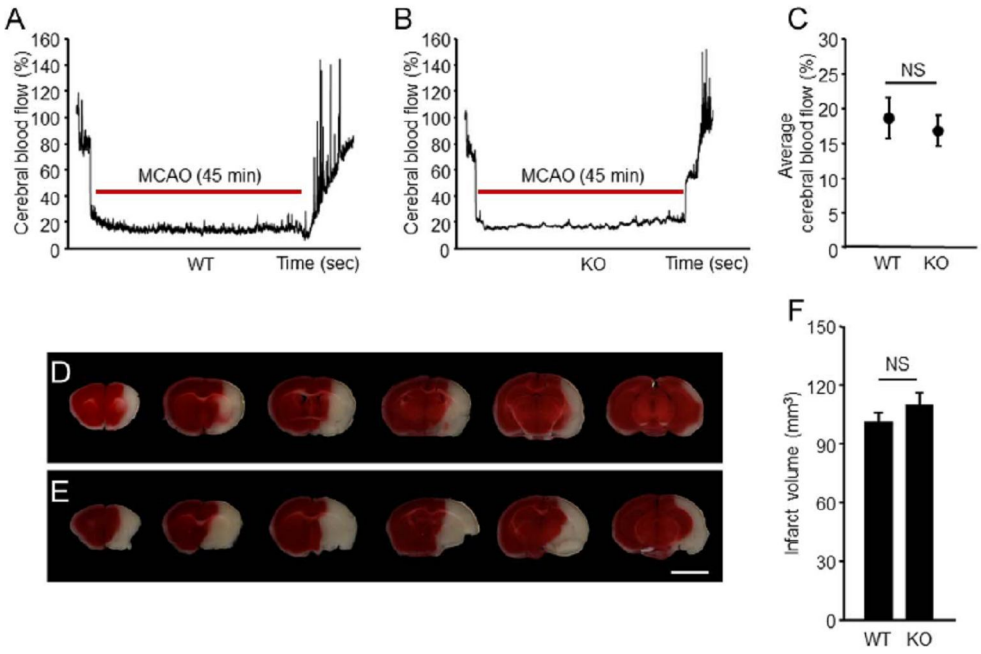

Cerebral blood flow and infarct volume after transient MCAO in the *Il21r* KO mice. (A and B) Cerebral blood flow was monitored by Laser-Doppler during transient focal ischemia (ligation) for 45 min both *Il21r* WT (A) and (B) *Il21r* KO mice. **(C)** There was no significant difference in average cerebral blood flow between genotypes during transient focal ischemia. Eight animals for each genotype were analyzed. **(D and E)** Serial brain sections (1 mm) from *Il21r* WT (D) and *Il21r* KO (E) mice 24 h after transient MCAO. The infarct appears white after TTC staining. Scale bar: 5 mm. **(F)** The graph shows the infarct volume for 8 animals for each genotype. Values represent mean ± SEM.

Supplemental Figure 5

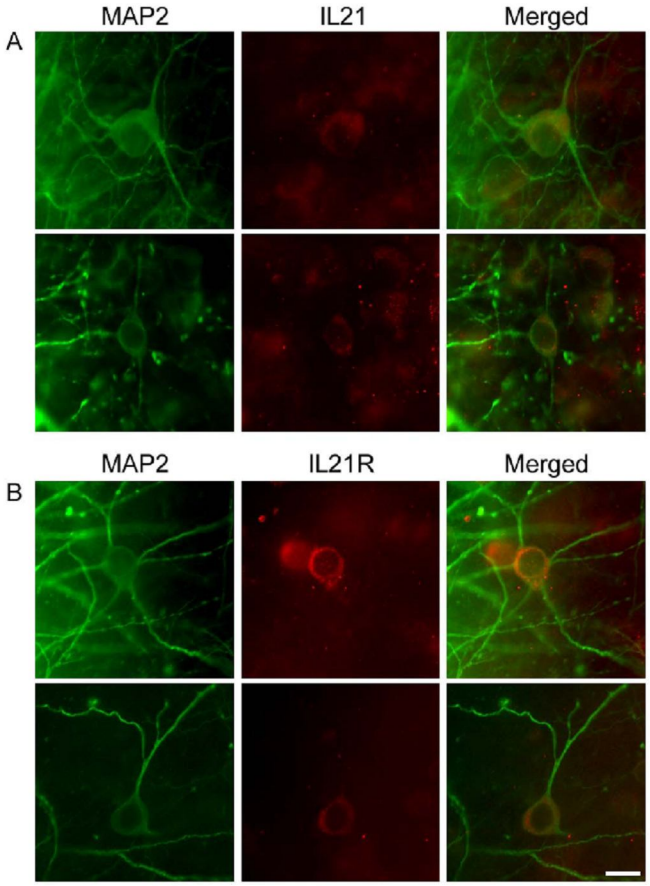

IL21 and IL21R are expressed on neurons in mouse brain slices. (A and B) Double immunofluorescence staining was performed using B6 mouse brain slices. Both IL21 (A) and IL21R (B) were stained with each specific antibody and indicated with red. Neurons were stained with MAP2 (microtubule associated protein 2) and indicated with green. Merged images show that IL21 and IL21R are expressed on neurons. Scale bar: 20 μm.

Supplemental Figure 6

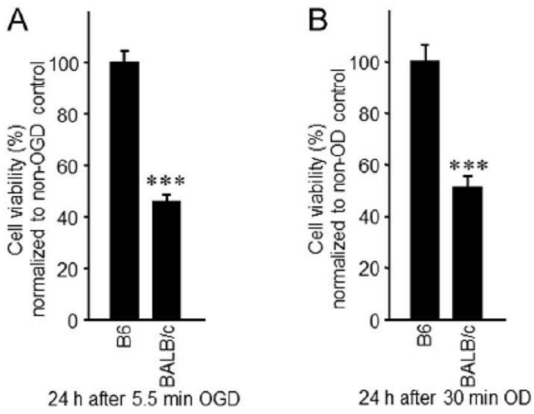

Neuronal cell death is nearly identical for ischemic stroke stimulation by either oxygen glucose deprivation (OGD) or oxygen deprivation (OD). (A and B) Two ex vivo ischemic stroke models, OGD (A) and OD (B), were compared using two inbred mouse strains, B6 and BALB/c. While the OD model allows the analysis of the *same* brain slice for both control and ischemic group (thus following the fate of each individual neuron before and after treatment), the OGD model requires *different* brain slices to be analyzed for the control and ischemic group (thus, following the fate of *different* brain slices, and therefore different neurons, in the treatment arms). In BALB/c, neuronal cell death was increased ~55% (A) and ~52% (B) compared to B6 with OGD (A) and OD (B), respectively. Experiments were performed three times using three to four mice per inbred strain for each experiment (Total number of animals: B6 (n=11) and BALB/c (n=14)). The number of the brain slices for B6 and BALB/c used 28 and 44 for OGD and 25 and 32 for OD, respectively. Values represent mean ± SEM (*** $p<.001$ *vs.* B6, by 2-tailed Student's *t* test).

Supplemental Figure 7

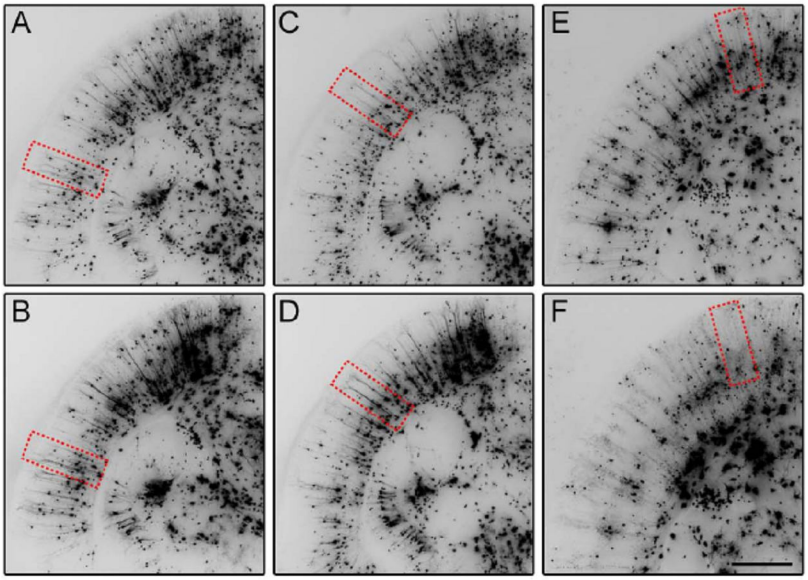

Cortical brain slices from wild type and *Il21r* mutant mice. (A – F) Cortical brain slices from each genotype were biolistically transfected with an YFP expression plasmid. The same brain slices for WT (A and B), Het (C and D), and KO (E and F) were monitored to analyze cell viability before (A, C, and E) and 24 h after oxygen deprivation (OD) (B, D, and F). The red boxes are magnified as representative images in Figure 3 (A – F). Scale bar: 1 mm.

Supplemental Figure 8

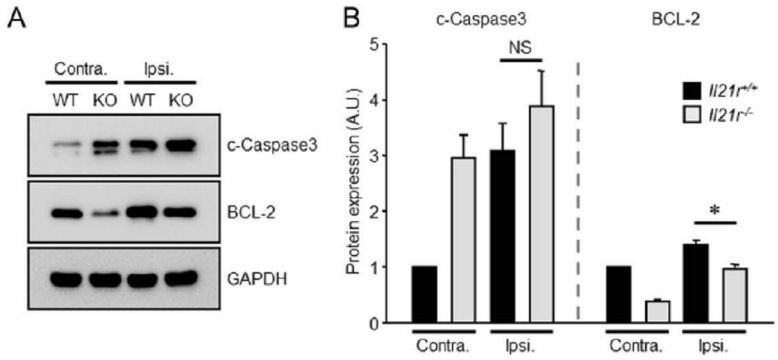

***Il21r* KO mice exhibit differences in cleaved Caspase 3 and BCL-2 protein after permanent MCAO. (A)** Western blots showing both cleaved Caspase 3 and BCL-2 from *Il21r* WT and *Il21r* KO mice 24 h after permanent MCAO. MCAO was performed on the right side of the brain (Ipsilateral) and the left side of the brain (Contralateral) was used as an internal control for both *Il21r* WT and *Il21r* KO mice. **(B)** Levels of cleaved Caspase3 and BCL-2 protein were determined using GAPDH for normalization. Experiments were performed with three mice per genotype. Values represent mean ± SEM (* $p<.05$, by 2-tailed Student's *t* test).

Supplemental Figure 9

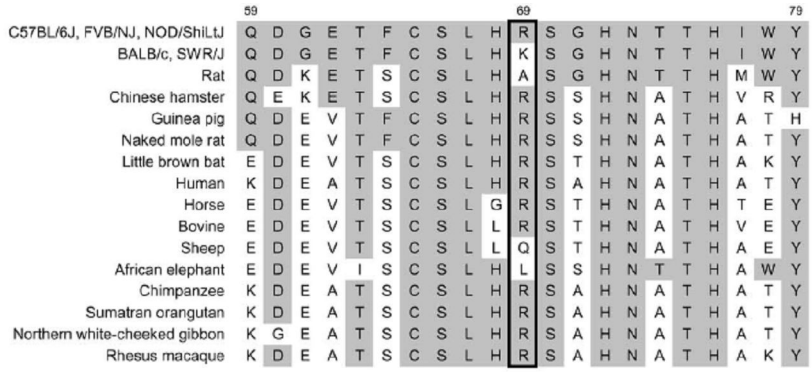

A non-synonymous coding SNP in *Il21r* gene. Alignments of a portion of amino acid sequences are compared across different inbred mouse strains and other mammalian species. The positions of relevant amino acid residues are indicated and sources of sequences are shown on the left. Grey boxes indicate conserved amino acid residues between inbred strains (B6, FVB, and NOD) showing small infarct volume and high number of vessel connections and the other species. The Arginine found at amino acid position 69 (rs33009726) in B6, FVB, and NOD mouse strains is conserved in some mammalian species, but variable in others. This R69K change is predicted to be functionally benign (Polyphen score: 0.039).

Supplemental Figure 10

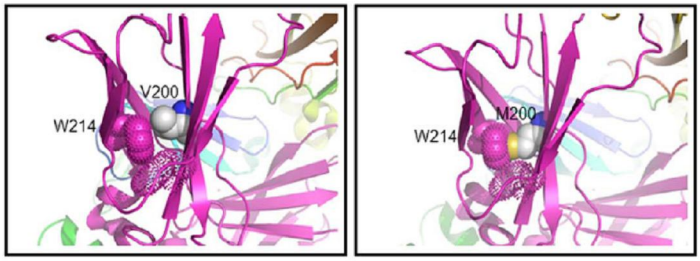

***In silico* structural analysis of the B6 (V200) and BALB/c (M200) IL21R protein. (A and B)** The predicted structure of the extracellular, second fibronectin domain for IL21R is shown for B6 (A) and BALB/c (B). A coding difference between B6 (V200) and BALB/c (M200) is located near the *WSXWS* motif (amino acid position 214 ~ 218), characteristic of class I cytokine receptors. Although the function(s) of this motif are not fully elucidated, it has been suggested to play a role in proper folding, export, receptor internalization, ligand binding, and signal transduction.

Supplemental Figure 11

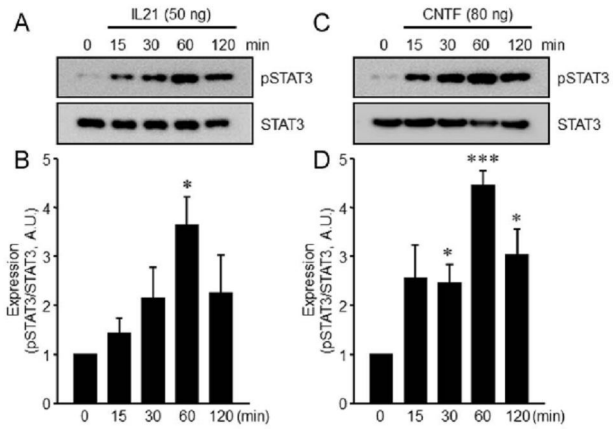

Quantitative measurement of pSTAT3 levels after treatment with recombinant cytokines. (A and C) A time course experiment was performed to identify the time of maximum downstream signaling after IL21 induction of explanted brain slices. Western blots are shown for both pSTAT3 and STAT3 after treatment of IL21 (50 ng/ml) (A) and CNTF (80 ng/ml) (C) in explanted brain slices of inbred mouse strain B6. **(B and D)** Levels of pSTAT3 were determined after treatment of IL21 and CNTF. The level of total STAT3 was used for normalization. pSTAT3 levels are maximal 1 h after treatment with IL21 and CNTF. Experiments were performed four times using three mice (B6) for each experiment. Values represent mean ± SEM (* *p<.05* and *** *p<.001 vs.* B6-vehicle treatment (0 h), by 2-tailed Student's *t* test).

Supplemental Figure 12

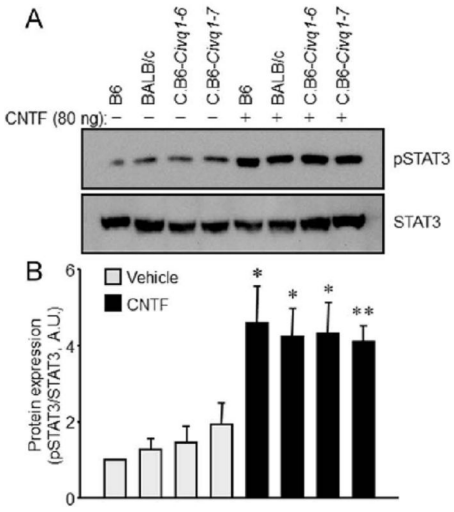

Signal transduction via CNTFR is not altered in different inbred mouse strains as well as two *Civq1* congenic lines after CNTF treatment. (A) Western blots were performed to detect both levels of pSTAT3 and STAT3 in explanted brain slices of two inbred mouse strains, B6 and BALB/c, as well as two *Civq1* congenic lines, C.B6-*Civq1-6* and C.B6-*Civq1-7*, 1 h after treatment of either vehicle or recombinant CNTF (80 ng/ml). **(B)** Level of pSTAT3 was determined. Level of STAT3 was used for normalization. Experiments were performed three times using three mice per mouse strain for each experiment. Values represent mean ± SEM (∗ *p<.05* and ∗∗ *p<.01 vs*. B6-vehicle treatment, by 2-tailed Student's *t* test).

Supplemental Figure 13

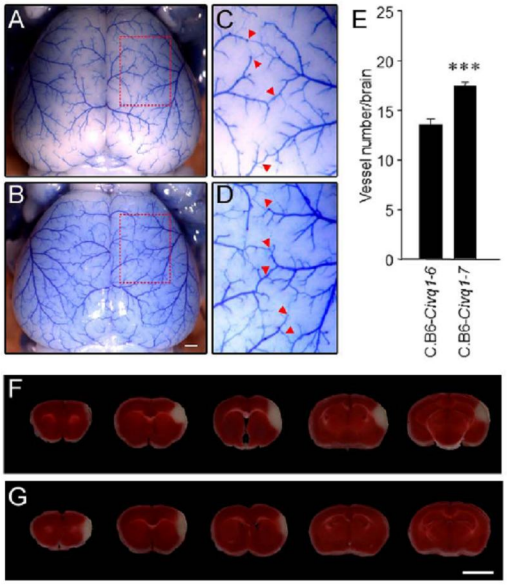

Collateral vessel anatomy on the pial surface of the cerebral cortex and infarct volume after MCAO in two *Civq1* congenic lines, C.B6-*Civq1-6* and C.B6-*Civq1-7*. (A and B) Representative images are shown for two *Civq1* congenic lines, C.B6-*Civq1-6* (A) and C.B6-*Civq1-7* (B). (Scale bar: 1 mm). **(C and D)** (C and D) are three times magnified from (A and B), respectively, and red arrowheads indicate vessel connections between the anterior cerebral artery (ACA) and the middle cerebral artery (MCA). **(E)** The graph indicates the average number of collateral vessel connections in the brain. The number of animals for C.B6-*Civq1-6* and C.B6-*Civq1-7* were 21 and 30 animals, respectively. Values represent mean ± SEM (*** *p<.001 vs.* C.B6-*Civq1-6*, by 2-tailed Student's *t* test). **(F and G)** Serial brain sections (1 mm) from C.B6-*Civq1-6* and C.B6-*Civq1-7* were measured infarction 24 h after MCAO. Infarct appears as white tissue after 2,3,5-Triphenyl-tetrazolium chloride (TTC) staining. Scale bar: 5 mm. The infarct volume is shown in Figure 5 (D).

Supplemental Figure 14

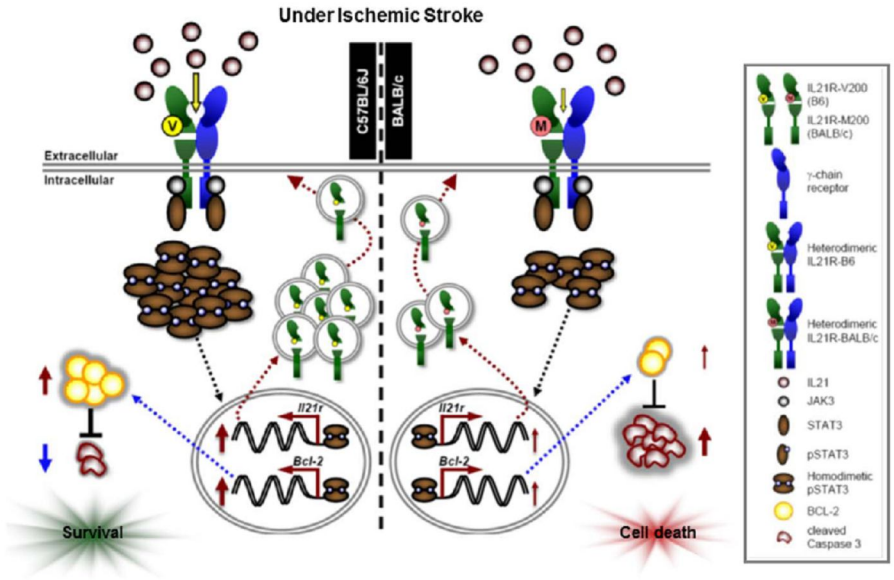

A schematic model of the role of IL21R in neuronal cell death caused by ischemic stroke. IL21R signal transduction differs between inbred mouse strains due to strain-specific gene expression and possibly a coding difference ($IL21R^{V200M}$). After ischemia, IL21R responsiveness is impaired in BALB/c, leading to reduced levels of pSTAT3. Lower levels of pSTAT3 result in different transcription levels of *Il21r* as well as lower levels of anti-apoptotic factor, BCL-2. In B6, increased levels and functionality of IL21R promotes increased STAT3 phosphorylation and increased BCL-2 which suppresses the Caspase 3 apoptotic pathway, leading to increased neuronal viability.

Supplemental Table 1

Gene symbol	Location (bp)	Gene name
4933440M02Rik	125,331,782 - 125,349,786	RIKEN cDNA 4933440M02 gene
Jmjd5 (Kdm8)	125,444,620 - 125,462,268	jumonji domain containing 5 (lysine (K)-specific demethylase 8)
Nsmce1	125,467,640 - 125,491,542	non-SMC element 1 homolog (S. cerevisiae)
Il4ra	125,552,282 - 125,579,474	interleukin 4 receptor, alpha
Il21r	125,603,429 - 125,633,570	interleukin 21 receptor
Gtf3c1	125,662,259 - 125,707,688	general transcription factor III C 1
Gsg1l	125,878,419 - 126,082,411	GSG1-like
Xpo6	126,118,471 - 126,200,408	exportin 6
Rabep2	126,438,370 - 126,446,476	rabaptin, RAB GTPase binding effector protein 2
Sept 1	127,214,442 - 127,218,445	septin 1
Itgal	127,296,260 - 127,335,137	integrin alpha L
Bcl7c	127,704,978 - 127,708,766	B cell CLL/lymphoma 7C

12 candidate genes within the shared SNP haplotype blocks for *Civq1* and *Canq1*.